



Contents lists available at ScienceDirect

Journal of Quantitative Spectroscopy & Radiative Transfer

journal homepage: www.elsevier.com/locate/jqsrt



Global climatology based on the ACE-FTS version 3.5 dataset: Addition of mesospheric levels and carbon-containing species in the UTLS



Ja-Ho Koo^a, Kaley A. Walker^{a,b,*}, Ashley Jones^{a,1}, Patrick E. Sheese^a,
Chris D. Boone^b, Peter F. Bernath^{b,c}, Gloria L. Manney^d

^a Department of Physics, University of Toronto, Toronto, Ontario, Canada

^b Department of Chemistry, University of Waterloo, Waterloo, Ontario, Canada

^c Department of Chemistry and Biochemistry, Old Dominion University, Norfolk, VA, USA

^d NorthWest Research Associates, and New Mexico Institute of Mining and Technology, Socorro, NM, USA

ARTICLE INFO

Article history:

Received 16 February 2016

Received in revised form

2 July 2016

Accepted 3 July 2016

Available online 7 July 2016

Keywords:

Trace gas climatology

Upper troposphere

Stratosphere

Mesosphere

Carbon-containing species

ACE-FTS

ABSTRACT

In this paper, we present a new climatology based on the Atmospheric Chemistry Experiment Fourier Transform Spectrometer (ACE-FTS) version 3.5 data set from February 2004 to February 2013. This extends the ACE-FTS climatology to include profile information in the mesosphere and carbon-containing species in the upper troposphere and lower stratosphere. Climatologies of 21 species, based on nine years of observations, are calculated, providing the most comprehensive and self-consistent climatology available from limb-viewing satellite measurements. Pressure levels from the upper troposphere to the mesosphere and lower thermosphere are included with ~ 3 to 4 km vertical resolution up to 10^{-4} hPa (~ 105 km). Volume mixing ratio values are filtered prior to the climatology estimation using the ACE-FTS data quality recommendations. The multi-year mean climatology contains zonal mean profiles for monthly and three-monthly (DJF, MAM, JJA, and SON) periods. These are provided with 5-degree spacing in either latitude or equivalent latitude. Also, the local daytime and nighttime distributions are provided separately for nitrogen-containing species, enabling diurnal differences to be investigated. Based on this climatology, examples of typical spatiotemporal patterns for trace gases in the mesosphere and for carbon-containing gases in the upper troposphere and lower stratosphere are discussed.

© 2016 Elsevier Ltd. All rights reserved.

1. Introduction

Climatologies of trace gases provide useful information to investigate the atmospheric environment and to understand the patterns resulting from atmospheric circulation and transport on a global scale. Climatological data sets provide

the zonal mean state of the atmosphere over a given time period as a function of latitude and altitude. In addition to being used to examine the typical characteristics of trace gases, these data sets can be utilized as a priori information for the retrieval of trace gases from ground-based spectral measurements [e.g. 1], to prescribe conditions in climate model simulations [e.g. 2] or to validate trace gas simulations [e.g. 3].

Recent chemistry-climate model validation activities, such as CCMVal (Chemistry-Climate Model Validation) [4] and CCMCI (Chemistry-Climate Model Initiative) [5], undertaken by

* Correspondence to: Department of Physics, University of Toronto, 60 St. George Street, Toronto, Ontario, Canada M5S 1A7.

E-mail address: kaley.walker@utoronto.ca (K.A. Walker).

¹ Now at, Chalmers University of Technology, Gothenburg, Sweden.

the SPARC (Stratosphere-troposphere Processes And their Role in Climate) project of the World Climate Research Program (WCRP) have highlighted the need for trace gas and aerosol climatologies from limb-sounding satellites for model evaluation. To better characterize the existing climatologies for these model validation activities, the SPARC Data Initiative has performed a comparison of climatologies obtained from satellite measurements over the past several decades [6]. Summaries of the results for the climatologies of O₃ [7,8], H₂O [9], and some halogen-containing species [10] have been published during this project. Also, studies were made to characterize and evaluate the impact of sampling biases for the climatologies produced in the project [11,12].

Prior to the SPARC Data Initiative, climatological datasets were developed from measurements by a number of limb-viewing satellites. A review of these trace gas climatologies is provided in Jones et al. [13]. As the focus of this paper is multi-species climatologies, the following discussion highlights studies in this area. The Halogen Occultation Experiment (HALOE) mission was the first to provide a comprehensive climatology for stratospheric O₃, H₂O, CH₄, NO_x, HCl, and HF [14]. The Michelson Interferometer for Passive Atmospheric Sounding (MIPAS) measurements have contributed stratospheric climatologies for many different species including CCl₃F (CFC-11) and CCl₂F₂ (CFC-12) [15]. Measurements by the Global Ozone Monitoring by Occultation of Stars (GOMOS) instrument were used to calculate a climatology for O₃, NO₂, and NO₃ [16] in the stratosphere and lower mesosphere. While the Superconducting Submillimeter-wave Limb-Emission Sounder (SMILES) provided data for less than a year, its multi-species climatology for O₃, HNO₃, HCl, ClO, HOCl, BrO, and HO₂ is quite useful because of the large altitude range, up to a maximum of 100 km [17]. The Atmospheric Chemistry Experiment Fourier Transform Spectrometer (ACE-FTS) has produced the most comprehensive climatology to date with a data set (from version 2.2) that includes 14 gas species and NO_y for the upper troposphere and stratosphere [13,18].

More recently, efforts have focused on combining data sets from different satellite instruments to produce merged data sets and climatologies. For example, the Global OZone Chemistry And Related trace gas Data records for the Stratosphere (GOZCARDS) project utilized data from the Stratospheric Aerosol and Gas Experiments (SAGE I and SAGE II), HALOE, the Microwave Limb Sounder (MLS) instruments on the Upper Atmosphere Research Satellite (UARS) and Aura platforms and ACE-FTS to produce merged monthly mean fields for O₃, HCl, H₂O, HNO₃, N₂O, NO, and NO₂ [19]. Combining data from SAGE II, SAGE III, HALOE, UARS MLS and Aura MLS, the Stratospheric Water and OzOne Satellite Homogenized (SWOOSH) database provides merged climatologies for O₃ and H₂O [20,21].

Following the SPARC Data Initiative activity, there were areas identified where additions and improvements could be made to the climatological data sets that are produced from the ACE-FTS measurements. Most limb-sounding measurements capture stratospheric properties, but have more limited coverage in the upper and lower atmosphere. Trace gas measurements in the mesosphere and thermosphere can be valuable for examining the Earth's climate [e.g. 22] and the influence of energetic particles on the Earth's atmosphere [e.g. 23–26]. Also, a climatology

covering the mesosphere and thermosphere can be useful for a priori or comparison data for ground-based measurements [e.g. 27] or global model simulations [e.g. 28]. Another issue that was identified was the limited amount of information about carbon-containing trace gases in the multi-species climatologies created to date. Climatologies of carbon-containing species are important for understanding the chemical environment of the upper troposphere and lower stratosphere (UTLS).

The ACE-FTS measurements, using the solar-occultation technique, provide atmospheric profiles over a wide altitude range from the upper troposphere to the lower thermosphere. The high signal-to-noise ratio and long path length of these measurements allow chemical species having low concentrations to be observed. Building on these advantages, we have calculated a new ACE-FTS climatology that includes trace gases measured in the mesosphere and lower thermosphere and carbon-containing species in the UTLS. The latest data version and nearly one decade of data from ACE-FTS have been used for this climatology. This work broadens the availability of trace gas climatology information for climate research. The paper is laid out as follows. In Section 2, the current ACE-FTS version 3.5 data set is described. The climatology calculation methods are detailed in Section 3 with the results for the new mesospheric levels and for the carbon-containing species presented in Section 4. Finally, a summary is provided in Section 5.

2. Data description

ACE-FTS is the infrared solar-occultation instrument onboard the Canadian SCISAT satellite launched on 12 August 2003 [29,30]. The ACE Measurement of Aerosol Extinction in the Stratosphere and Troposphere Retrieved by Occultation (ACE-MAESTRO) [31] and two-channel visible/near-infrared imager (ACE-IMAGER) [32] are also carried on SCISAT with ACE-FTS. The SCISAT satellite was launched into an orbit at 650 km altitude with a 74-degree inclination angle to the equator, producing the highest density of measurements over high latitude regions. ACE-FTS can make up to 15 sunrise and 15 sunset observations every day and covers all global latitudes from 85°N to 85°S approximately every three months (over each year). There are short gaps in measurements (~every three months) where the satellite's orbit geometry is such that the Sun remains in full view of the instrument for a couple of weeks, yielding no occultations.

For the calculation of this climatology, we use the version 3.5 ACE-FTS data set that is available from February 2004 to February 2013 [33]. Vertical profiles of 38 species and 26 additional isotopologues are retrieved from the spectra measured in the infrared region (between 750 and 4400 cm⁻¹) at a spectral resolution of 0.02 cm⁻¹ [29]. To retrieve the volume mixing ratio (VMR) of each species, pressure and temperature information is required [34]. Vertical profiles of pressure and temperature are retrieved (by utilizing CO₂ features in narrow microwindows) for altitudes between 15 and 125 km, but fixed to meteorological data from the Canadian Meteorological Centre (CMC) [35,36] or the data from the NRLMSISE-00 model

[37] for the lowest or highest altitudes outside of this range, respectively. These pressure and temperature profiles are then employed with the spectral line information from the HITRAN 2004 database [38] with updates for the VMR retrieval. All profiles are provided on the tangent height (as measured) grid and interpolated onto a uniform 1-km grid based on a piecewise quadratic method [34]. The vertical resolution of the ACE-FTS measurements is 3–4 km based on the instrument field-of-view and the vertical sampling varies between ~1.5 and 6 km depending on the angle between the satellite's orbital plane and the look direction to the Sun. Approximately 32,000 measurements were used for the climatology calculation. The data quality flags used to filter the data for outliers (version 1.1) are provided with the ACE-FTS version 3.5 data set [39].

The v3.5 ACE-FTS retrievals differ from the earlier v2.2 dataset primarily in three areas. First, there has been an improvement to the pressure/temperature retrievals that lead to a reduction in unphysical oscillations in the temperature profiles produced. Second, the microwindow sets have been updated for all of the retrieved trace gases and the number of interfering species allowed in the retrievals has been increased. Finally, five species have been included in the VMR retrievals (namely, COCl₂, COClF, H₂CO, CH₃OH, and HCFC-141b) and two have been removed (HOCl and ClO).

The version 3.0/3.5 VMR profiles from ACE-FTS measurements have been validated through comparisons with ground-based [e.g. 40], balloon [e.g. 41], and other satellite measurements [e.g. 42]. Detailed descriptions of validation results for the earlier version 2.2 data set were summarized in Jones et al. [13] and comparisons between version 2.2 and version 3.0/3.5 were described by Waymark et al. [43]. The changes in the ACE-FTS profiles with v3.5 were generally found to reduce biases identified in the v2.2 data set [43]. Compared to coincident satellite observations (within 350 km and 3 h), ACE-FTS v3.5 temperatures agree to within ± 2 K between 15 and 40 km, within ± 7 K between 40 and 80 km and within ± 12 K between 80 and 100 km (P. Sheese, personal communication).

3. Methodology

Jones et al. [13,18] produced the first ACE-FTS climatology using five years of measurements for 14 species plus NO_y from the version 2.2 dataset. In the current work, we have used the version 3.5 dataset over a longer (nine year) measurement period. In addition to the baseline species (O₃, H₂O, CH₄, N₂O, CO, NO, NO₂, N₂O₅, HNO₃, ClONO₂, CCl₃F, CCl₂F, and HF) considered in Jones et al. [13], seven carbon-containing species (C₂H₆, C₂H₂, HCN, CH₃OH, HCOOH, H₂CO, and OCS) are newly added to this climatology. In addition, an updated methodology has been employed as described below.

A climatology, providing atmospheric mean state information on a global scale, is often used for initial or boundary conditions in model simulations or for model comparisons. To facilitate this, the ACE-FTS climatology is calculated on atmospheric pressure coordinates. Starting

from the levels used for the SPARC CCMVal activity [4], 28 pressure levels were selected below 0.1 hPa level for the ACE-FTS climatology: 300, 250, 200, 170, 150, 130, 115, 100, 90, 80, 70, 50, 30, 20, 15, 10, 7, 5, 3, 2, 1.5, 1, 0.7, 0.5, 0.3, 0.2, 0.15, 0.1 hPa. In this work, the vertical range for the climatology is extended up to 10⁻⁴ hPa (~105 km) to utilize the ACE-FTS measurements in the mesosphere and lower thermosphere. For this, 15 additional pressure levels were selected from 0.1 to 10⁻⁴ hPa: 0.08, 0.05, 0.03, 0.02, 0.01, 0.007, 0.004, 0.003, 0.002, 0.001, 0.0008, 0.0005, 0.0003, 0.0002, 0.0001 hPa by considering the levels used in the Whole Atmosphere Community Climate Model (WACCM) [44]. These newly added levels are spaced by approximately 3–4 km, the vertical resolution of the ACE-FTS instrument. ACE-FTS measurements of O₃, CO, CH₄, NO, N₂O, and H₂O extend above the stratosphere and these results will be discussed further in Section 4.1.

Before starting the climatology calculation, the data quality flags are used to remove potentially unreliable data [39]. Only VMR data with flags 0 and 1 were used for the calculation. For profiles containing flags 4 to 7, which correspond to unnatural outliers, the entire profile is removed. For VMR values with flags 2 or 3, where statistical analysis was not possible [39], the VMR value at that altitude is removed. Compared to using the median absolute deviation (MAD) [45], the data filtering process based on the ACE-FTS quality flags can provide a more reliable climatology [39].

After this quality check, the VMR profiles are interpolated to the pressure level grid for the climatology using a spline fitting method. Then they are grouped based on a monthly or three-monthly basis for preparing the mean profiles. Finally, these grouped VMR profiles are divided into spatial bins (at each pressure level) with 5-degree latitude spacing (e.g. 90°S–85°S, 85°S–80°S, etc.). Due to the strong influence of the polar vortex in high latitude regions, it is often useful to sort VMRs using vortex-relative coordinates. Therefore, we also compile the VMR data using 5-degree bins in equivalent latitude, a vortex-centered coordinate based on the potential vorticity [46]. Equivalent latitudes are obtained from the Derived Meteorological Products (DMPs), provided for the time and location of each measurement [47]. It should be noted that the potential vorticity information only extends up to ~70 km, so the equivalent latitude climatologies are limited to an upper height of ~0.01 hPa. The DMP version used here is based on GEOS-5.1.0 and GEOS-5.2.0 [48]. Finally, the set of multi-year mean zonal mean profiles are calculated by averaging all of the interpolated VMR values for each pressure level within each of the latitude or equivalent latitude bins. A minimum of five data points is required for each calculated level and bin. The total number of data points used for each pressure and latitude bin calculation is provided with the climatological fields. As noted above, this is done for either a single month or a three-month period. While each one-month climatology does not have global coverage (due to the high inclination angle of the SCISAT orbit), the three-month climatology provides nearly global coverage and generally captures the seasonal variation [13]. It should be noted that these three-month fields are not strictly seasonal averages because

ACE-FTS only samples certain latitudes during any given month [18]. While ACE-FTS does have an annually repeating pattern of measurement latitudes, this variation in measurement latitudes with time could give rise to sampling biases as discussed in [11]. Since some species show strong diurnal variation (e.g., NO, NO₂, HNO₃, N₂O₅, ClONO₂), we also calculate individual climatologies for AM (before local solar noon) and PM (after local solar noon) separately by using the local solar time of each measurement as described by Jones et al. [13]. The local sunrise and sunset times of the ACE-FTS measurements vary with latitude over the year as shown in Fig. 3 of [18]. Because of this, mean and median local solar time information is provided with the AM and PM climatological fields. When the multi-year zonal mean profiles are calculated, the standard deviation is also calculated for each pressure and latitude bin, providing information about the variability of the VMRs. Finally, to provide an uncertainty estimate for the zonal mean profiles, the average of the statistical fitting error (as described in [34]) for all of the data points in each pressure and latitude bin is calculated. This process was also applied to the ACE-FTS temperature profiles and this climatology is included in the data set.

4. Results

In this section, we briefly describe the climatologies for several trace gases as examples of this new dataset. To highlight the changes and additions for the v3.5 ACE-FTS climatology, we discuss (1) the trace gas features in the

mesosphere and lower thermosphere (Section 4.1) (2) the distributions of non-methane carbon-containing species in the UTLS (Section 4.2). For the comparison of the spatial distribution and seasonal variation of species, we use the vertical mean profile for six latitudinal ranges, 60°N–90°N, 30°N–60°N, 30°S–30°N, 60°S–30°S, 90°S–60°S, and 90°S–90°N: These are the polar and midlatitude regions for the Northern Hemisphere (NH), the polar and midlatitude regions for the Southern Hemisphere (SH), the Tropics, and all latitudes. The results shown are based on three-month combined climatologies and standard deviations for December–January–February (DJF) and June–July–August (JJA), accompanied by figures illustrating the vertical profiles for the six latitude ranges.

4.1. Trace gas climatologies for the mesosphere

ACE-FTS ozone (O₃) climatology is compared for two seasons, DJF and JJA (Fig. 1), with profiles reaching to 0.0005 hPa pressure at the uppermost level. The stratospheric O₃ peak VMR has a maximum of ~10 ppbv in the tropics in DJF with a global (90°S–90°N) mean value at this height of approximately 8 ppbv. Owing to more frequent perturbations due to wave activity and dynamical variability in the Arctic, the winter stratospheric ozone peak is higher in the NH than the SH (Fig. 1b and e). In the mesosphere, the climatology shows the ozone increase from 0.01 hPa to the secondary peak in ozone near 0.001 hPa. The mesospheric O₃ peak is fairly consistent between the NH and SH in DJF, but this peak is slightly higher in the NH in JJA [e.g. 49–51].

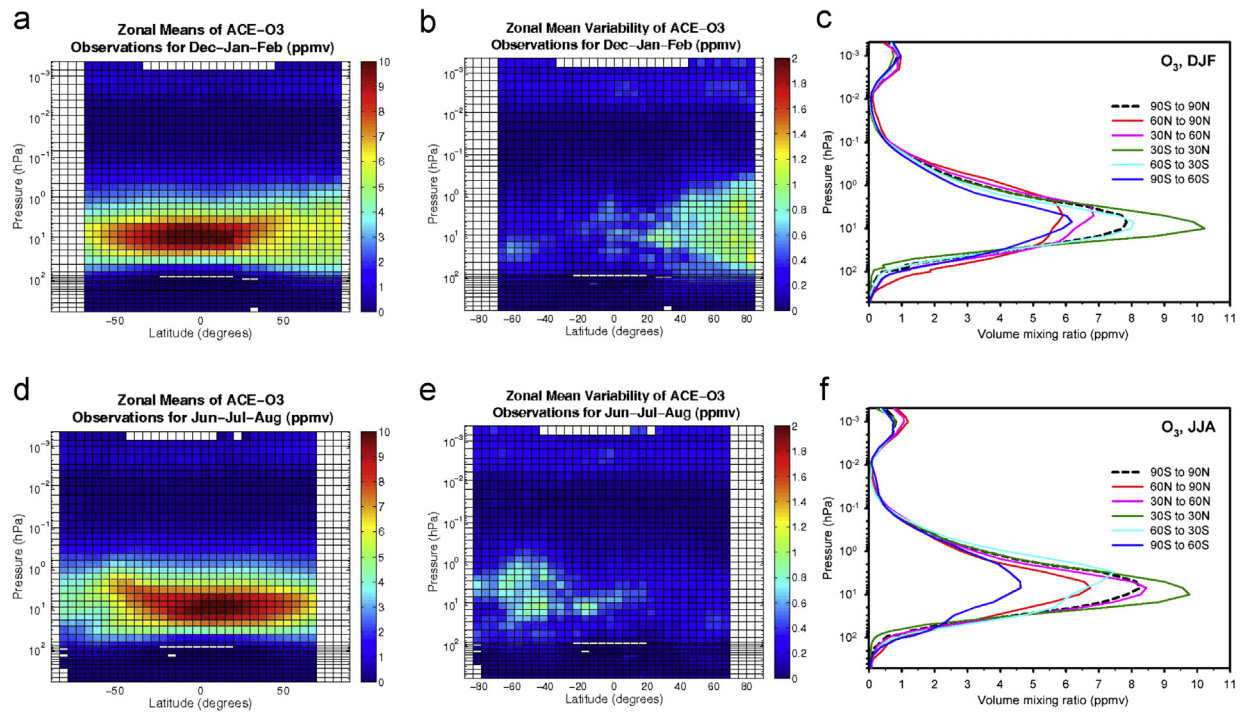


Fig. 1. ACE-FTS three-month climatology of O₃ for (a) December–January–February (DJF) and (d) June–July–August (JJA). One sigma standard deviation of the climatology is also shown for (b) DJF and (e) JJA. In addition, the zonal mean profiles for six latitude ranges (60°N–90°N, 30°N–60°N, 30°S–30°N, 60°S–30°S, 90°S–60°S, and 90°S–90°N) are compared for (c) DJF and (f) JJA.

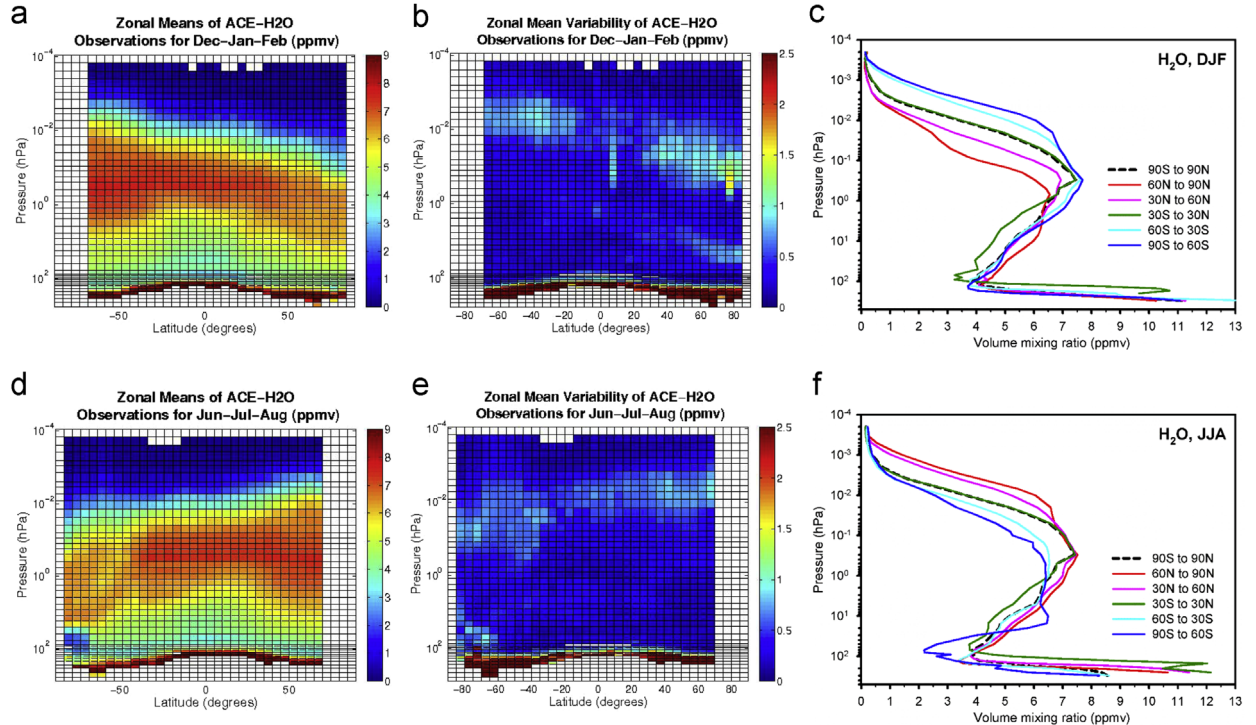


Fig. 2. Same as Fig. 1 but for H₂O.

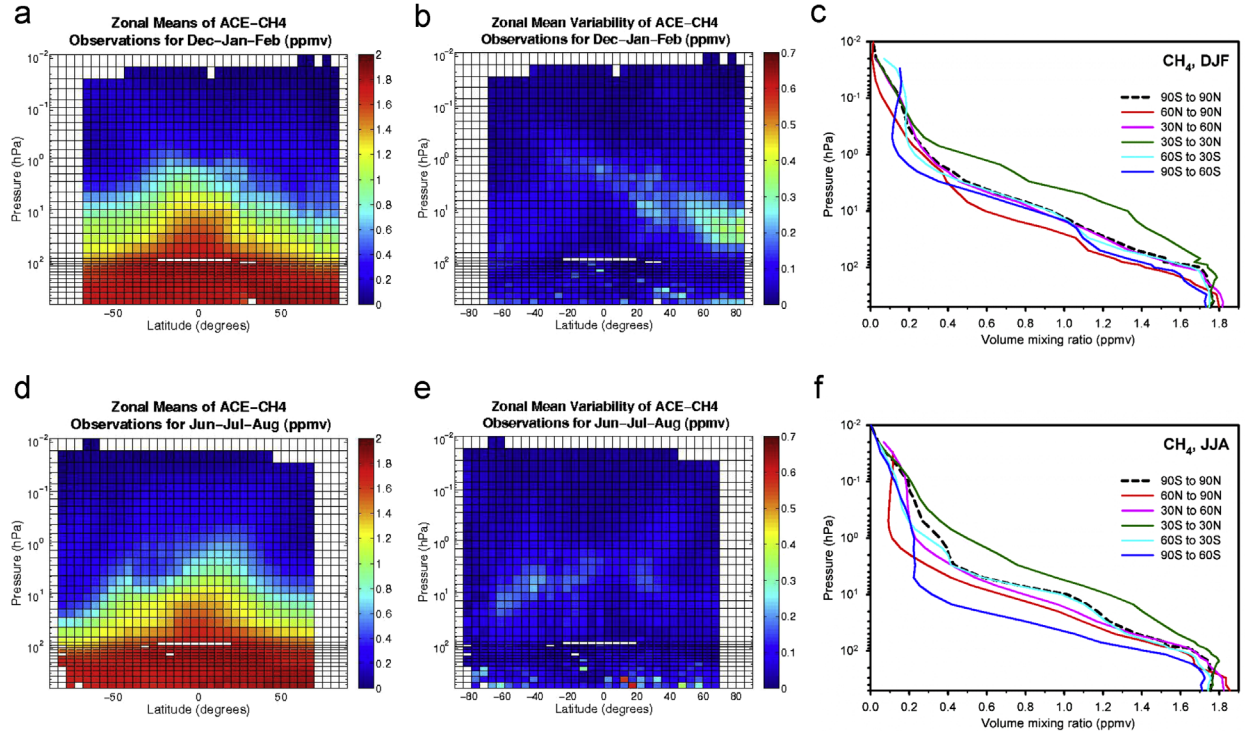


Fig. 3. Same as Fig. 1 but for CH₄.

Fig. 2 shows the comparison of the DJF and JJA climatologies for water vapor (H₂O). In the lower altitudes, the variation of the hygropause with latitude can be seen

in **Fig. 2a** and **d** (also in the wider latitude range means in **Fig. 2c** and **f**). Upper tropospheric H₂O decreases with altitude because of the decrease in saturation vapor

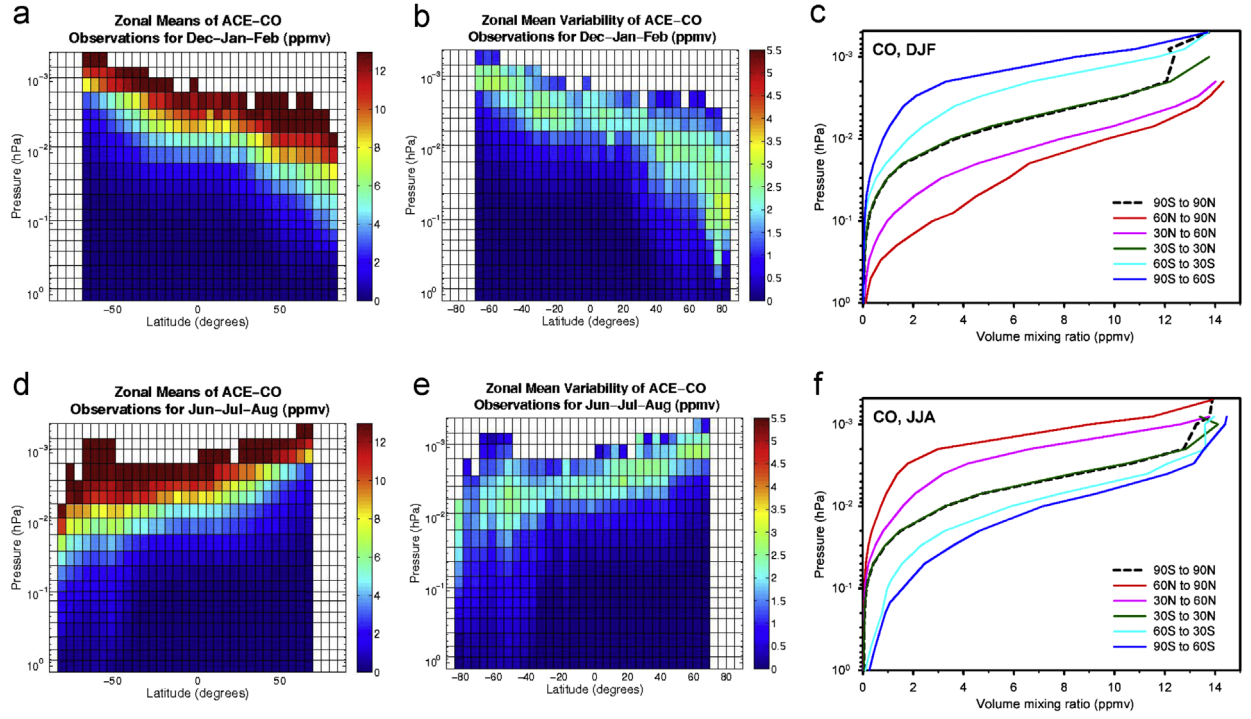


Fig. 4. Same as Fig. 1 but for CO at heights above 1 hPa.

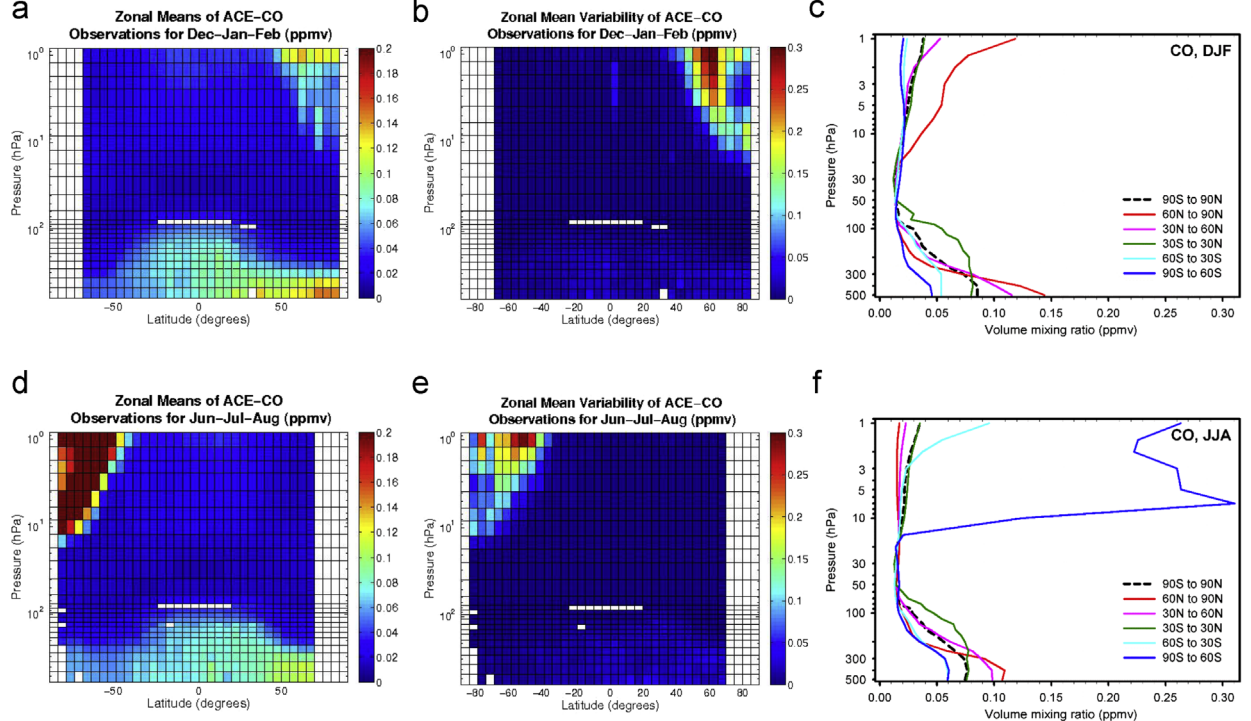


Fig. 5. Same as Fig. 1 but for CO at heights below 1 hPa. Note, in panel f, the extreme values in the winter 90–60S zonal mean profile (above 20 hPa) result from descent of CO from the upper atmosphere (c.f. high latitude SH zonal mean profiles in panel d).

pressure with decreasing temperature. In the stratosphere, H₂O has a photochemical source from the oxidation of CH₄, therefore the VMR increases with increasing altitude and

is anti-correlated with CH₄. In the mesosphere, H₂O is photolyzed by Lyman-alpha radiation (121.6 nm), resulting in decreasing VMR with increasing altitude [52]. The

maximum VMR appears at the lowest measured altitudes, with values higher than 10 ppmv, and a peak in VMR of about 7 ppmv in the upper stratosphere. In the winter hemisphere, we can see the pattern of air-mass descent from the mesosphere into the stratosphere. This strong descent typically occurs when there is a strong polar vortex in the upper stratosphere and lower mesosphere [e.g. 53–56].

Methane (CH_4) zonal mean distributions for DJF and JJA are shown in Fig. 3. The maximum height of the CH_4 climatology is 0.01 hPa, (lower than that for the O_3 and H_2O data sets). The main sources of CH_4 include emissions from wetlands and anthropogenic activity such as leaks from natural gas installations and from livestock at the surface. CH_4 shows a maximum value throughout the upper troposphere of ~ 1.7 ppmv that has a fairly uniform distribution with latitude. There is a rapid decrease with increasing height because of oxidation in the stratosphere (as mentioned above). As shown in the H_2O climatology, lower stratospheric CH_4 VMRs can be seen in the winter hemisphere due to the strong descent from the mesosphere, consistent with previous results [57 and references therein]. Regions showing higher variability (standard deviations) are also well matched with these regions of descent (Fig. 3b and e), with more variation from year-to-year in the NH.

The next example shown is for carbon monoxide (CO). Since the scale of CO variation in the upper and lower atmosphere is quite different, the upper and lower atmospheric CO climatologies are shown in two figures and are discussed separately. In Fig. 4, climatologies for DJF and JJA are compared from 1 to 0.0001 hPa and Fig. 5 shows the

DJF and JJA climatologies for up to 1 hPa. Fig. 4 shows the strong increase in CO in the upper mesosphere and lower thermosphere due to the chemical production by CO_2 photolysis [22]. The vertical extent of CO-rich air masses illustrates the descent of mesospheric air to the stratosphere in the winter hemisphere (Fig. 4a and d) [e.g. 54]. Furthermore, there is a significant variation in this descent between years, which is shown in the large standard deviation of the VMRs (Fig. 4b and e). This wintertime descent provides a large CO difference between NH and SH of ~ 10 ppmv in the mesosphere and illustrates the utility of using CO for monitoring upper atmospheric dynamics [58,59].

4.2. Climatologies of non-methane carbon-containing species in the UTLS

In this section, we focus on example climatologies that are primarily for the UTLS region. In Fig. 5, the CO climatology for heights lower than 1 hPa is shown for DJF and JJA. As shown in Fig. 4, enriched CO from the upper atmosphere can reach as low as the middle stratosphere in the winter hemisphere [e.g. 60]. In the upper troposphere, CO concentrations are greater in the NH than in the SH. This hemispheric CO asymmetry is due to differences in the sources of the surface emissions. The maximum in upper tropospheric CO appears in DJF in the NH because of large natural and anthropogenic emissions from the continents and slow chemical loss processes in the wintertime [e.g. 61,62].

Unlike CO and CH_4 , the VMRs of other carbon-containing species are retrieved from ACE-FTS

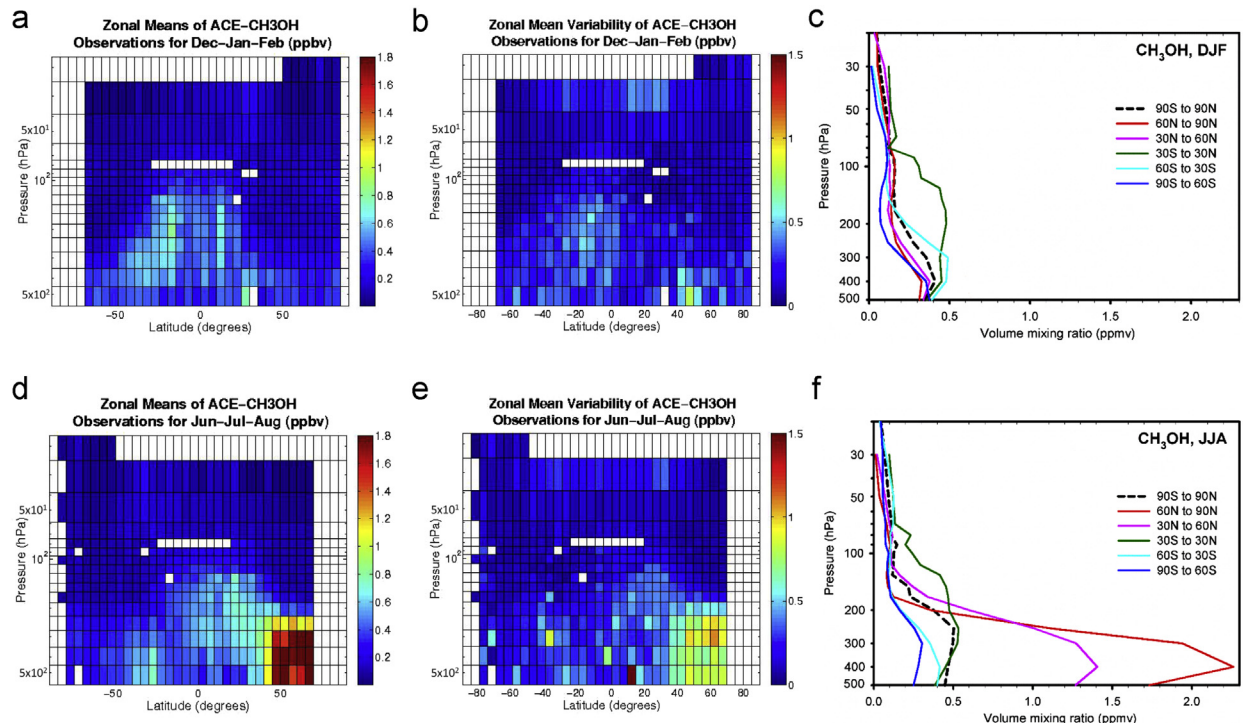


Fig. 6. Same as Fig. 1 but for CH_3OH .

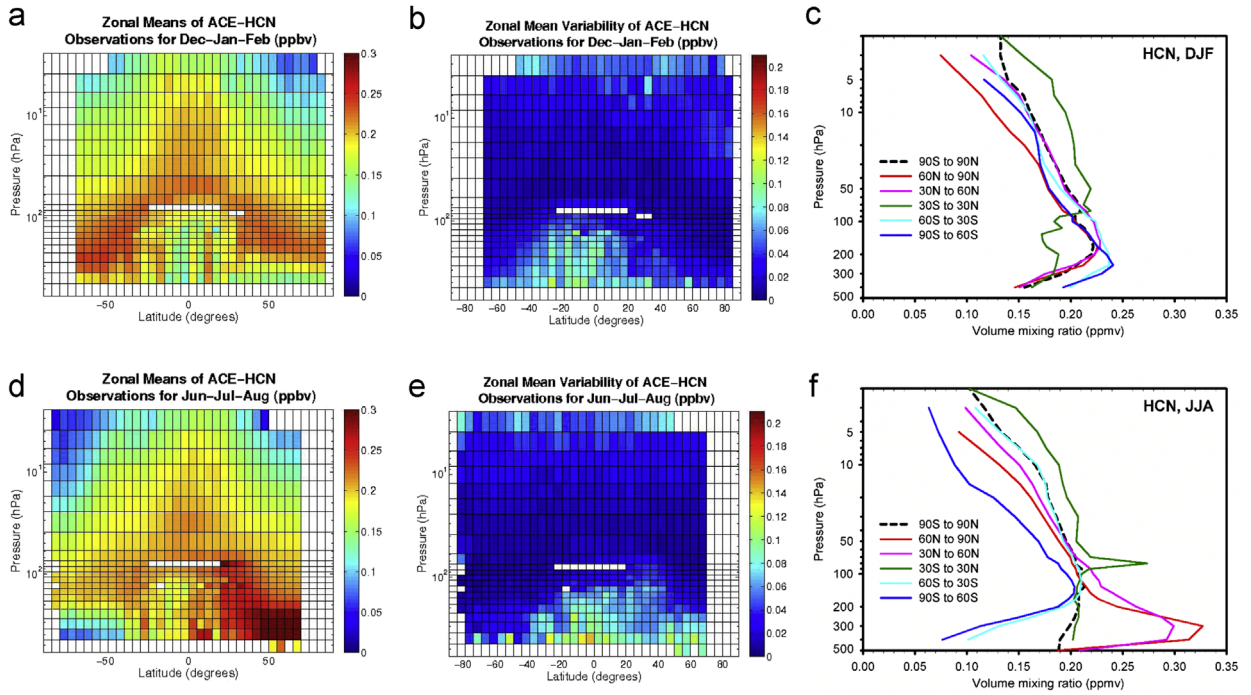


Fig. 7. Same as Fig. 1 but for HCN.

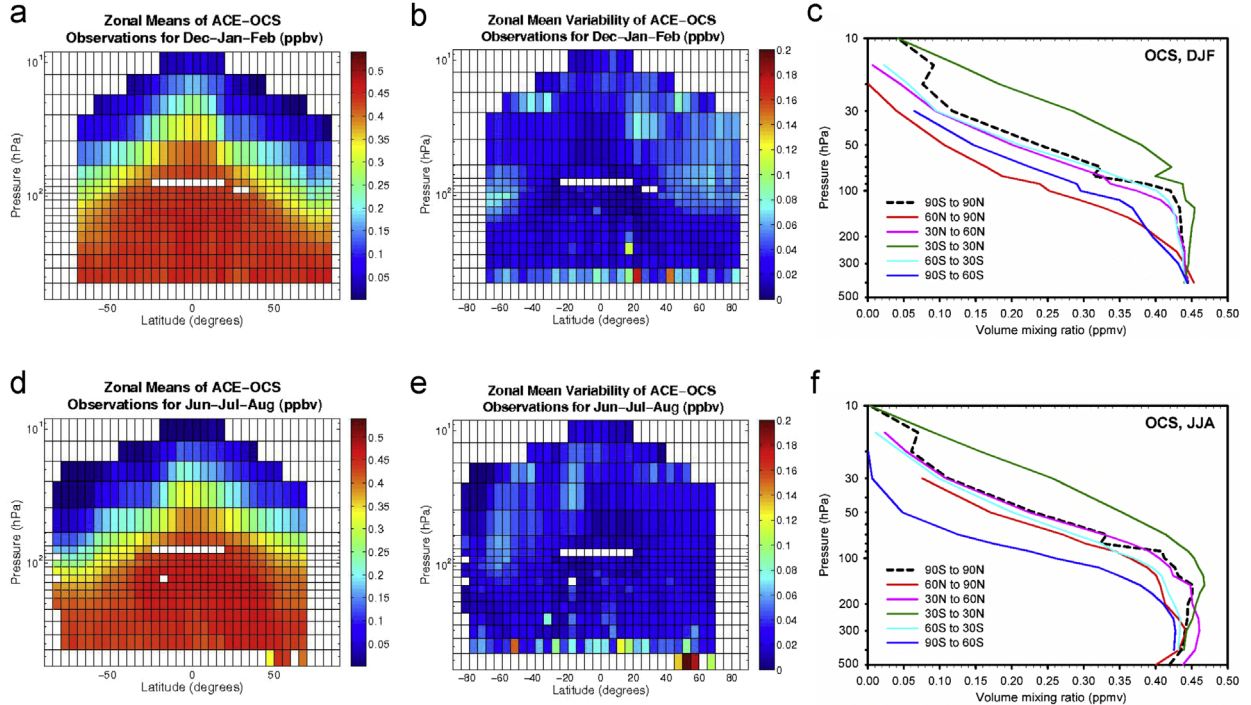


Fig. 8. Same as Fig. 1 but for OCS.

measurements only in the UTLS. Thus the top height of these climatologies is lower than 1 hPa. Methanol (CH_3OH) is the next example and is shown in Fig. 6. In the troposphere, CH_3OH is the second most abundant hydrocarbon species after methane and it is primarily generated by the growth and decay of plants and by biomass burning.

CH_3OH also plays a role as a significant chemical source for formaldehyde (H_2CO) and CO [63]. The climatology shows a VMR range from 0 to 2 ppbv, and there is a high standard deviation in the region with the highest VMR values. There is little production of tropospheric CH_3OH during DJF while there is much higher production during JJA

particularly over the NH. This seasonal pattern is anti-correlated with tropospheric CO (shown in Fig. 5) and has been discussed in some field studies [e.g. 64]. While it is possible that this difference arises from the different sources for these species, more research will be required in the future to understand this relationship. CH₃OH also shows high VMRs in the upper troposphere (100–200 hPa level) in the tropics (30°S–30°N) that may be due to vertical transport.

Fig. 7 shows the hydrogen cyanide (HCN) climatology for DJF and JJA. Owing to its longer chemical lifetime, ~4 years [e.g. 62, 65–67], HCN is relatively well mixed in the upper troposphere globally and it is also transported into the lower stratosphere (Fig. 7a and d). Over the tropics, HCN can reach up to the 1 hPa level. The global mean HCN VMR is ~0.1–0.2 ppbv. Because HCN is emitted from biomass and biofuel burning regions, it generally shows higher zonal mean VMRs and standard deviations in the summer hemisphere (JJA in NH, and DJF in SH). The ocean surface plays a role as a sink of HCN [e.g. 62, 66, 67] and, as a result, it can impact the HCN VMRs at the lowest levels of the climatology in seasons when the emissions are lower (Fig. 7c and f). It should be noted that the quasi-biannual “tape recorder” signal in HCN found in [66] and explained in [68] is damped in this multi-year average climatology.

The final example of a carbon-containing species is carbonyl sulfide (OCS) (Fig. 8). In contrast to HCN, the ocean surface is the main source of OCS through direct outgassing or chemical production by the oxidation of carbon disulfide and dimethyl sulfide emitted from the ocean [69]. Owing to its wide source area and relatively long lifetime (2–6 years), OCS is quite well-mixed in the upper troposphere with VMRs of ~0.4 to 0.5 ppbv, little horizontal and vertical gradient in the VMRs and weak seasonality (Fig. 8c and f). This is also shown as low variability in the standard deviations of the VMRs. OCS can also be injected into the lower stratosphere through tropical convection reaching up to 10 hPa. Above these heights, OCS becomes rapidly photo-dissociated by UV radiation or destroyed by reaction with OH [69].

5. Summary

This study describes the process used to estimate new monthly and three-monthly ACE-FTS climatologies using the version 3.5 dataset. This work provides a consistent climatological dataset for 21 species (including several carbon-containing trace gases) averaged over a nine-year period with a wide vertical range, from the upper troposphere to the lower thermosphere. In addition, newly available data quality filtering has been applied to improve the reliability of the climatologies. It provides zonal mean data binned by latitude or equivalent latitude as well as climatologies separated on the basis of the local time of the measurements for nitrogen-containing species.

We also presented examples of the spatial distributions and seasonal differences for different trace gases using these climatologies. The mesospheric/lower thermospheric climatologies showed different phenomena such as air-mass descent in polar winter and the effect of

photochemistry for certain species. Also, the climatologies of carbon-containing species demonstrated how the spatiotemporal variation can be captured. These can be used to examine the influence of chemical sources or sinks and associated atmospheric chemical processes in the UTLS. The version 3.5 ACE-FTS climatology is available as a supplement to this paper and from the ACE Mission Website (<http://www.ace.uwaterloo.ca/>).

Acknowledgments

This work was supported by grants from the Natural Sciences and Engineering Research Council of Canada (NSERC). The Atmospheric Chemistry Experiment (ACE), also known as SCISAT, is a Canadian-led mission mainly supported by the Canadian Space Agency (CSA) and NSERC. We thank Adam Marr for his assistance in preparing the supplementary data files.

References

- [1] Vigouroux C, De Mazière M, Demoulin P, Servais C, Hase F, Blumenstock T, et al. Evaluation of tropospheric and stratospheric ozone trends over Western Europe from ground-based FTIR network observations. *Atmos Chem Phys* 2008;8:6865–86.
- [2] Son S-W, Gerber EP, Perlitz J, Polvani LM, Gillett NP, Seo K-H, et al. Impact of stratospheric ozone on southern hemisphere circulation change: A multimodel assessment. *J Geophys Res* 2010. <http://dx.doi.org/10.1029/2010JD014271>.
- [3] Tilmes S, Lamarque J-F, Emmons LK, Conley A, Schultz MG, Saunois M, et al. Technical note: Ozonesonde climatology between 1995 and 2011 description, evaluation and applications. *Atmos Chem Phys* 2012;12:7475–97.
- [4] SPARC CCMVal, SPARC report on the evaluation of chemistry-climate models. Eyring V, Shepherd TG, Waugh DW, editors. SPARC report no. 5, WCRP-132, WMO/TD-No. 1526; 2010.
- [5] Hegglin MI, Lamarque J-F, Eyring V, Hess P, Young PJ, Fiore AM, Myhre G, Nagashima T, Ryerson T, Shepherd TG, Waugh DW. IGAC/SPARC Chemistry-Climate Model Initiative (CCMI). 2014 Science workshop, SPARC newsletter; 2014. p. 43.
- [6] SPARC Data Initiative. SPARC report on the evaluation of trace gas and aerosol climatologies from satellite limb sounders. Hegglin MI and Tegtmeier S, editors; 2016 (In preparation).
- [7] Tegtmeier S, Hegglin MI, Anderson J, Bourassa A, Brohede S, Degenstein D, et al. SPARC Data Initiative: a comparison of ozone climatologies from international satellite limb sounders. *J Geophys Res* 2013;118:12229–47. <http://dx.doi.org/10.1002/2013JD019877>.
- [8] Neu JL, Hegglin MI, Tegtmeier S, Bourassa A, Degenstein D, Froidevaux L, et al. The SPARC data initiative: comparison of upper troposphere/lower stratosphere ozone climatologies from limb-viewing instruments and the nadir-viewing Tropospheric Emission Spectrometer. *J Geophys Res* 2014;119:6971–90. <http://dx.doi.org/10.1002/2013JD020822>.
- [9] Hegglin MI, Tegtmeier S, Anderson J, Froidevaux L, Fuller R, Funke B, et al. SPARC data initiative: comparison of water vapor climatologies from international satellite limb sounders. *J Geophys Res* 2013;118:11824–46. <http://dx.doi.org/10.1002/jgrd.50752>.
- [10] Tegtmeier S, Hegglin MI, Anderson J, Funke B, Gilje J, Jones A, et al. The SPARC data initiative: comparisons of CFC-11, CFC-12, HF and SF₆ climatologies from international satellite limb sounders. *Earth Syst Sci Data* 2016;8:61–78. <http://dx.doi.org/10.5194/essd-8-61-2016>.
- [11] Toohey M, Hegglin MI, Tegtmeier S, Anderson J, Añel JA, Bourassa A, et al. Characterizing sampling biases in the trace gas climatologies of the SPARC data initiative. *J Geophys Res* 2013;118:11847–62. <http://dx.doi.org/10.1002/jgrd.50874>.
- [12] Toohey M, von Clarmann T. Climatologies from satellite measurements: the impact of orbital sampling on the standard error of the mean. *Atmos Meas Tech* 2013;6:937–48. <http://dx.doi.org/10.5194/amt-6-937-2013>.

- [13] Jones A, Walker KA, Jin JJ, Taylor JR, Boone CD, Bernath PF, et al. Technical note: a trace gas climatology derived from the Atmospheric Chemistry Experiment Fourier Transform Spectrometer (ACE-FTS) data set. *Atmos Chem Phys* 2012;12:5207–20.
- [14] Grooß J-U, Russell JM. Technical note: a stratospheric climatology for O₃, H₂O, CH₄, NO_x, HCl and HF derived from HALOE measurements. *Atmos Chem Phys* 2005;5:2797–807.
- [15] Kellmann S, von Clarmann T, Stiller GP, Eckert E, Glatthor N, Höpfner MH, et al. Global CFC-11 (CCl₃F) and CFC-12 (CCl₂F₂) measurements with the Michelson Interferometer for Passive Atmospheric Soundings (MIPAS): retrieval, climatologies and trends. *Atmos Chem Phys* 2012;12:11857–75. <http://dx.doi.org/10.5194/acp-12-11857-2012>.
- [16] Kyrölä E, Tamminen J, Sofieva V, Bertaux JL, Hauchecorne A, Lalaurier F, et al. GOMOS O₃, NO₂, and NO₃ observations in 2002–2008. *Atmos Chem Phys* 2010;10:7723–38. <http://dx.doi.org/10.5194/acp-10-7723-2010>.
- [17] Kreyling D, Sagawa H, Wohltmann I, Lehmann R, Kasai Y. SMILES zonal and diurnal variation climatology of stratospheric and mesospheric trace gasses: O₃, HCl, HNO₃, ClO, BrO, HOCl, HO₂, and temperature. *J Geophys Res* 2013;118:11888–903. <http://dx.doi.org/10.1002/2012JD019420>.
- [18] Jones A, Qin G, Strong K, Walker KA, McLinden CA, Toohey M, et al. A global inventory of stratospheric NO_y from ACE-FTS. *J Geophys Res* 2011;116:D17304. <http://dx.doi.org/10.1029/2010JD015465>.
- [19] Froidevaux L, Anderson J, Wang H-J, Fuller RA, Schwartz MJ, Santee ML, et al. Global Ozone Chemistry And Related trace gas Data records for the Stratosphere (GOZCARDS): methodology and sample results with a focus on HCl, H₂O, and O₃. *Atmos Chem Phys* 2015;15: 10471–507. <http://dx.doi.org/10.5194/acp-15-10471-2015>.
- [20] Tummon F, Hassler B, Harris NRP, Staehelin J, Steinbrecht W, Anderson J, et al. Intercomparison of vertically resolved merged satellite ozone data sets: interannual variability and long-term trends. *Atmos Chem Phys* 2015;15:3021–43. <http://dx.doi.org/10.5194/acp-15-3021-2015>.
- [21] Davis SM, et al. The Stratospheric Water and Ozone Satellite Homogenized (SWOOSH) database: a long-term database for climate studies, manuscript under review. *Earth Syst Sci Data Discuss* 2016. <http://dx.doi.org/10.5194/essd-2016-16>.
- [22] Emmert JT, Stevens MH, Bernath PF, Drob DP, Boone CD. Observations of increasing carbon dioxide concentration in Earth's thermosphere. *Nat Geosci* 2012;5:868–71. <http://dx.doi.org/10.1038/NGEO1626>.
- [23] Randall CE, Harvey VL, Bailey S, Singleton CS, Bernath P, Boone C, et al. Energetic particle precipitation effects on the southern hemisphere stratosphere in 1992–2005. *J Geophys Res* 2007;112: D08308. <http://dx.doi.org/10.1029/2006JD007696>.
- [24] Randall CE, Harvey VL, Siskind DE, France J, Bernath PF, Boone CD, et al. NO_x descent in the Arctic middle atmosphere in early 2009. *Geophys Res Lett* 2009;36:L18811. <http://dx.doi.org/10.1029/2009GL039706>.
- [25] Andersson MÉ, Verronen PT, Rodger CJ, Clilverd MA, Seppälä. Missing driver in the Sun-Earth connection from energetic electron precipitation impacts mesospheric ozone. *Nat Commun* 2014;5: 5197. <http://dx.doi.org/10.1038/ncomms6197>.
- [26] Funke B, López-Puertas M, Stiller GP, von Clarmann T. Mesospheric and stratospheric NO_y produced by energetic particle precipitation during 2002–2012. *J Geophys Res Atmos* 2014;119:4429–46. <http://dx.doi.org/10.1002/2013JD021404>.
- [27] Hoffmann CG, Raffalski U, Palm M, Funke B, Golchert SHW, Hochschild G, et al. Observation of strato-mesospheric CO above Kiruna with ground-based microwave radiometry – retrieval and satellite comparison. *Atmos Meas Tech* 2011;4:2389–408. <http://dx.doi.org/10.5194/amt-4-2389-2011>.
- [28] Pendlebury D, Plummer D, Scinocca J, Sheese P, Strong K, Walker K, et al. Comparison of the CMAM30 data set with ACE-FTS and OSIRIS: polar regions. *Atmos Chem Phys* 2015;15:12465–85. <http://dx.doi.org/10.5194/acp-15-12465-2015>.
- [29] Bernath PF, McElroy CT, Abrams MC, Boone CD, Butler M, Camy-Peyret C, et al. Atmospheric Chemistry Experiment (ACE): mission overview. *Geophys Res Lett* 2005;32:L15S01. <http://dx.doi.org/10.1029/2005GL022386>.
- [30] Bernath PF. The Atmospheric Chemistry Experiment (ACE). *J Quant Spectrosc Radiat Transf* 2016 (submitted for this issue).
- [31] McElroy CT, Nowlan CR, Drummond JR, Bernath PF, Barton DV, Dufour DG, et al. The ACE-MAESTRO instrument on SCISAT: description, performance, and preliminary results. *Appl Opt* 2007;46:4341–56.
- [32] Gilbert KL, Turnbull DN, Walker KA, Boone CD, McLeod SD, Butler M, et al. The onboard imagers for the Canadian ACE SCISAT-1 mission. *J Geophys Res* 2007;112:D12207. <http://dx.doi.org/10.1029/2006JD007714>.
- [33] Boone CD, Walker KA, Bernath PF. Version 3 Retrievals for the Atmospheric Chemistry Experiment Fourier Transform Spectrometer (ACE-FTS), The Atmospheric Chemistry Experiment ACE at 10: A solar occultation anthology. Virginia USA: A Deepak publishing; 2013.
- [34] Boone CD, Nassar R, Walker KA, Rochon YJ, McLeod SD, Rinsland CP, et al. Retrievals for the atmospheric chemistry experiment fourier-transform spectrometer. *Appl Opt* 2005;44:7218–31.
- [35] Côté JS, Gravel S, Méthot A, Patoine A, Roch M, Staniforth A. The operational CMC-MRB global environmental multiscale (GEM) model. Part I: design considerations and formulations. *Mon Weather Rev* 1998;126:1373–95.
- [36] Gauthier PC, Charette C, Fillion L, Koclás P, Laroche S. Implementation of a 3D variational data assimilation system at the Canadian Meteorological Centre. Part I: The global analysis. *Atmos Ocean* 1999;37:103–56.
- [37] Picone JM, Hedin AE, Drob DP, Aikin AC. NRLMSISE-00 empirical model of the atmosphere: statistical comparisons and scientific issues. *J Geophys Res* 2002;107:1468–83.
- [38] Rothman LS, Jacquemart D, Barbe A, Benner DC, Birk M, Brown LR, et al. The HITRAN 2004 molecular spectroscopic database. *J Quant Spectrosc Radiat Transf* 2005;96:139–204.
- [39] Sheese PE, Boone CD, Walker KA. Detecting physically unrealistic outliers in ACE-FTS atmospheric measurements. *Atmos Meas Tech* 2015;8:741–50. <http://dx.doi.org/10.5194/amt-8-741-2015>.
- [40] Adams C, Strong K, Batchelor RL, Bernath PF, Brohede S, Boone C, et al. Validation of ACE and OSIRIS ozone and NO₂ measurements using ground-based instruments at 80°N. *Atmos Meas Tech* 2012;5: 927–53. <http://dx.doi.org/10.5194/amt-5-927-2012>.
- [41] Velázco VA, Toon GC, Blavier JFL, Kleinböhl A, Manney GL, Daffer WH, et al. Validation of the Atmospheric Chemistry Experiment by noncoincident MkIV balloon profiles. *J Geophys Res* 2011;116:D06306. <http://dx.doi.org/10.1029/2010JD014928>.
- [42] Sheese PE, Walker KA, Boone CD, Bernath PF, Froidevaux L, Funke B, Raspolini P, Von Clarmann T. ACE-FTS ozone, water vapour, nitrous oxide, nitric acid, and carbon monoxide profile intercomparisons with MIPAS and MLS. Accepted by *J Quant Spectrosc Radiat Transf* (for this special issue), 16 June 2016.
- [43] Waymark C, Walker KA, Boone CD, Bernath PF. ACE-FTS version 3.0 data set: validation and data processing update. *Ann Geophys* 2013;56. <http://dx.doi.org/10.4401/ag-6339>.
- [44] Marsh DR, Mills MJ, Kinnison DE, Lamarque J-F, Calvo N, Polvani LM. Climate change from 1850 to 2005 simulated in CESM1(WACCM). *J Clim* 2013;26:7372–91. <http://dx.doi.org/10.1175/JCLI-D-12-00558.1>.
- [45] Toohey M, Strong K, Bernath PF, Boone CD, Walker KA, Jonsson AI, et al. Validating the reported random errors of ACE-FTS measurements. *J Geophys Res* 2010;115:D20304.
- [46] Butchart N, Remsberg EE. The area of the stratospheric polar vortex as a diagnostic for tracer transport on an isentropic surface. *J Atmos Sci* 1986;43:1319–39.
- [47] Manney GL, Daffer WH, Zawodny JM, Bernath PF, Hoppel KW, Walker KA, et al. Solar occultation satellite data and derived meteorological products: sampling issues and comparisons with Aura Microwave Limb Sounder. *J Geophys Res* 2007;112:D24S50. <http://dx.doi.org/10.1029/2006JD008709>.
- [48] Rienecker M, Suarez M, Todling R, Bacmeister J, Takacs L, Liu H-C, Gu W, Sienkiewicz M, Koster R, Gelaro R, Stajner I, Nielsen J. The GEOS-5 data assimilation system – documentation of versions 5.0.1, 5.1.0, and 5.2.0. In: . Suarez MJ, editors. Technical report series on global modeling and data assimilation vol. 27, NASA, 10 NASA/TM-2008-104606, Greenbelt, MD, USA, 13207:1-101; 2008.
- [49] Evans WFJ, Llewellyn Ej. Measurements of mesospheric ozone from observations of the 127 μ band. *Radio Sci* 1972;7:45–50.
- [50] Hays PB, Roble RG. Observation of mesospheric ozone at low latitudes. *Planet Space Sci* 1973;21:273–97.
- [51] Kaufmann M, Gusev OA, Grossmann KU, Martín-Torres FJ, Marsh DR, Kutepov AA. Satellite observations of daytime and nighttime ozone in the mesosphere and lower thermosphere. *J Geophys Res* 2003;108:4272. <http://dx.doi.org/10.1029/2002JD002800>.
- [52] Remsberg E. Observed seasonal to decadal scale responses in mesospheric water vapor. *J Geophys Res* 2010;115:D06306. <http://dx.doi.org/10.1029/2009JD012904>.
- [53] Randall CE, Harvey VL, Singleton CS, Bernath PF, Boone CD, Kozyra JU. Enhanced NO_x in 2006 linked to strong upper stratospheric Arctic vortex. *Geophys Res Lett* 2006;33:L18811. <http://dx.doi.org/10.1029/2006GL027160>.
- [54] Manney GL, Schwartz MJ, Krüger K, Santee ML, Pawson S, Lee JN, et al. Aura Microwave Limb Sounder observations of dynamics and

- transport during the record-breaking 2009 Arctic stratospheric major warming. *Geophys Res Lett* 2009;36:L12815. <http://dx.doi.org/10.1029/2009GL038586>.
- [55] Orsolini YJ, Urban J, Murtagh DP, Lossow S, Limpasuvan V. Descent from the polar mesosphere and anomalously high stratopause observed in 8 years of water vapor and temperature satellite observations by the Odin Sub-Millimeter Radiometer. *J Geophys Res* 2010;115:D12305. <http://dx.doi.org/10.1029/2009JD013501>.
- [56] Lahoz WA, Errera Q, Viscardy S, Manney GL. The 2009 stratospheric major warming described from synergistic use of BASCOE water vapour analyses and MLS observations. *Atmos Chem Phys* 2011;11: 4689–703. <http://dx.doi.org/10.5194/acp-11-4689-2011>.
- [57] Minschwaner K, Manney GL. Derived methane in the stratosphere and lower mesosphere from Aura Microwave Limb Sounder measurements of nitrous oxide, water vapor, and carbon monoxide. *J Atmos Chem* 2014;71:253–67. <http://dx.doi.org/10.1007/s10874-015-9299-z>.
- [58] McDonald AJ, Smith M. A technique to identify vortex air using carbon monoxide observations. *J Geophys Res Atmos* 2013;118: 12,719–33. <http://dx.doi.org/10.1002/2012JD019257>.
- [59] Harvey VL, Randall CE, Collins RL. Chemical definition of the mesospheric polar vortex. *J Geophys Res Atmos* 2015;120: 10,166–79. <http://dx.doi.org/10.1002/2015JD023488>.
- [60] Jin JJ, Semeniuk K, Beagley SR, Fomichev VI, Jonsson AI, McConnell JC, et al. Comparison of CMAM simulations of carbon monoxide (CO), nitrous oxide (N_2O), and methane (CH_4) with observations from Odin/SMR, ACE-FTS, and Aura/MLS. *Atmos Chem Phys* 2009;9: 3233–52. <http://dx.doi.org/10.5194/acp-9-3233-2009>.
- [61] Hegglin MI, Boone CD, Manney GL, Walker KA. A global view of the extratropical tropopause transition layer from Atmospheric Chemistry Experiment Fourier Transform Spectrometer O_3 , H_2O , and CO. *J Geophys Res* 2009;114:D00B11. <http://dx.doi.org/10.1029/2008JD009984>.
- [62] Park M, Randel WJ, Kinnison DE, Emmons LK, Bernath PF, Walker KA, et al. Hydrocarbons in the upper troposphere and lower stratosphere observed from ACE-FTS and comparisons with WACCM. *J Geophys Res* 2013;118:1–17. <http://dx.doi.org/10.1029/2012JD018327>.
- [63] Jacob DJ, Field BD, Li Q, Blake DR, de Gouw J, Warneke C, et al. Global budget of methanol: constraints from atmospheric observations. *J Geophys Res* 2005;110:D08303. <http://dx.doi.org/10.1029/2004JD005172>.
- [64] Viatte C, Strong K, Walker KA, Drummond JG. Five years of CO, HCN, C_2H_6 , C_2H_2 , CH_3OH , $HCOOH$, and H_2CO total columns measured in the Canadian high Arctic. *Atmos Meas Tech* 2014;7: 1547–70. <http://dx.doi.org/10.5194/amt-7-1547-2014>.
- [65] Pumphrey HC, Jimenez CJ, Waters JW. Measurement of HCN in the middle atmosphere by EOS MLS. *Geophys Res Lett* 2006;33: L08804. <http://dx.doi.org/10.1029/2005GL025656>.
- [66] Pumphrey HC, Boone C, Walker KA, Bernath P, Livesey NJ. Tropical tape recorder observed in HCN. *Geophys Res Lett* 2008;35: L05801. <http://dx.doi.org/10.1029/2007GL032137>.
- [67] Li Q, Palmer PI, Pumphrey HC, Bernath P, Mahieu E. What drives the observed variability of HCN in the troposphere and lower stratosphere? *Atmos Chem Phys* 2009;9:8531–43.
- [68] Pommrich R, Müller R, Grooß J-U, Günther G, Konopka P, Riese M, et al. What causes the irregular cycle of the atmospheric tape recorder signal in HCN? *Geophys Res Lett* 2010;37: L16805. <http://dx.doi.org/10.1029/2010GL044056>.
- [69] Barkley MP, Palmer PI, Boone CD, Bernath PF, Suntharalingam P. Global distributions of carbonyl sulfide in the upper troposphere and stratosphere. *Geophys Res Lett* 2008;35:L14810. <http://dx.doi.org/10.1029/2008GL034270>.